34th Annual International Conference of the IEEE EMBS
San Diego, California USA, 28 August - 1 September, 2012

Surface Deformation Tracking of a Silicone Gel Skin Phantom in Response to Normal Indentation

Matthew D. Parker[1], Mihailo Azhar, Thiranja P. Babarenda Gamage, Darren Alvares, Andrew J. Taberner, Poul M. F. Nielsen

Abstract—**Identifying the mechanical properties of the skin has been the subject of much study in recent years, as such knowledge can provide insight into wound healing, wrinkling and minimization of scarring through surgical planning.**

Traditional experimental methods used to extract mechanical properties in vivo, such as suction/torsion tests are not capable of measuring the skin's anisotropic mechanical properties.

We have previously developed a 3D force-sensitive micro-robot to induce controlled, complex deformation patterns, allowing characterization of the anisotropic properties of skin. This paper describes the introduction of a three-camera stereoscope to measure the strain field of the deforming surface on a soft silicone gel phantom, using three-dimensional Phase Cross Correlation (PCC) methods on a speckle pattern.

I. Introduction

Human skin is a nonlinear, anisotropic and viscoelastic material [1–5]. Quantitative measurement of these properties would be of use in surgical planning to minimise scarring [6], developing appropriate treatment paths for chronic and acute wounds [7], testing the efficacy of cosmetics, and measuring the state of health of the tissue [8].

Numerous deformation tests have been used to extract material properties *in-vivo* [9–11], but most require simplifying assumptions, such as a linear force-displacement relationship, elastic, or isotropic behaviour. These assumptions can lead to significant inaccuracies, limiting the usefulness of such models. In-plane deformation sets, such as those obtained using biaxial testing, or purely surface-normal indentation, cannot completely characterise the anisotropic properties of skin *in vivo*. To address this problem we have constructed a 3-axis microrobot to create significantly richer three-dimensional force-deformation profiles than has previously been possible [12], [13].

Manuscript received March 29, 2012. This work was supported by the New Zealand Ministry of Research Science and Technology's New Economy Research Fund.

M. D. Parker is with the Auckland Bioengineering Institute at The University of Auckland (phone: +64 9 373 7599; fax: +64 9 367 7157 ; e-mail: mpar145@aucklanduni.ac.nz).

M. Azhar is with the Auckland Bioengineering Institute at The University of Auckland (e-mail: mazh003@aucklanduni.ac.nz).

T. P. Babarenda Gamage is with the Auckland Bioengineering Institute at The University of Auckland (e-mail: psam012@aucklanduni.ac.nz).

A. J. Taberner is with the Auckland Bioengineering Institute and the Department of Engineering Science at The University of Auckland (e-mail: a.taberner@auckland.ac.nz).

P. M. F. Nielsen is with the Auckland Bioengineering Institute and the Department of Engineering Science at The University of Auckland (e-mail: p.nielsen@auckland.ac.nz).

Our microrobot uses a probe, attached to the skin with an adhesive, which can produce a rich set of three dimensional deformations. Force transducers measure the 3D reaction force vector at the probe tip while the 3D position of the probe is determined from three linear position transducers. The skin surface displacement is measured using multicamera stereoscopy. Experiments using this device promise to provide sufficient information to enable characterization of nonlinear, anisotropic, and time-varying skin properties [13].

This paper details the combination of our microrobot with a three-camera stereoscope in order to capture surface deformation measurements simultaneous with microrobot indentation tests. We present results from an initial surface deformation experiment on a silicone gel sample which his used to mimic skin. The setup has been designed for future use in *in-vivo* soft tissue experiments.

II. Methodology

Stereoscope Design

The Stereoscopic rig consists of three CMOS cameras (Photon Focus MVD1024E160CL), providing 1024 x 1024 pixel resolution, coupled with machine vision lenses (Fujion CF25HA-1). The cameras are mounted on aluminum blocks, oriented 55º to horizontal. Diffuse lighting of the imaging surface is supplied by a halogen-powered fiber optic ring illuminator. Camera control is operated via National Instruments' LabVIEW, using a synchronized CameraLink interface.

Fig. 1. Three-camera stereoscope fixed in place on solid aluminum blocks.

The microrobot is placed between the three cameras, so that the indenter is located on the same side as the imaging devices. Camera calibration was performed using a multi-

plane checkerboard direct calibration method using software developed at the University of Bonn [14].

A. Microrobot design

The 3D force-sensitive microrobot has been explained in depth by Flynn et al [12]. In brief, the microrobot uses three parallel axes, each driven by a voice coil to adjust the height of a corner of a moving platform. Atop the moving platform sit three force transducers, which are in turn attached to a

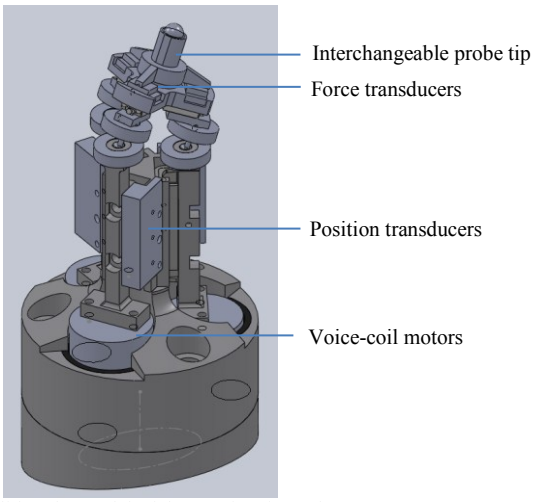

Fig. 2. Solidworks model of the 3-axis microrobot.

pyramidal probe. Linear position transducers provide a repeatability of 62µm and a sensitivity of about 0.5V/mm [12].

Real-time control of the microrobot is performed on a National Instruments CompactRIO controller (cRIO-9022), while probe tip positions are specified in a LabVIEW 2011 user interface.

B. Soft Material Phantom

Silicone gels have proved useful in simulated soft tissue experiments and validations of mechanical models, as they have well-defined material properties [15–17] . A 40 mm x 40 mm soft tissue phantom was constructed using Sylgard ® dielectric 527 silicone gel (Dow Corning, USA). The stiffness of the gel can be adjusted by controlling the ratio of the two liquids used to form it. A part A to part B ratio of 1:2 was used, as it allowed the microrobot tip to indent the silicone without puncturing it.

The two part mixture was placed in a vacuum chamber at -90 kPa, before curing at 40ºC. This process aimed to reduce heterogeneity in the gel by removing air bubbles.

C. Experimental Setup

The microrobot was placed on the base of the stereoscope with the probe tip extending upwards at equidistance from each camera. An acrylic sheet attached to the silicone phantom was placed above the microrobot, so that the tip could extend to and deform the phantom (Figure 3).

Images were taken with the probe outside of the field of view of the stereoscope, providing an occlusion-free set of images for initial material point identification.

The probe tip was then moved towards the gel until the force transducers recorded a noticeable increase of force. This position was defined as zero displacement. The probe tip was then extended in 100 µm increments, normal to the gel surface to a total displacement of 3000 µm. Image sets were taken at each increment in displacement.

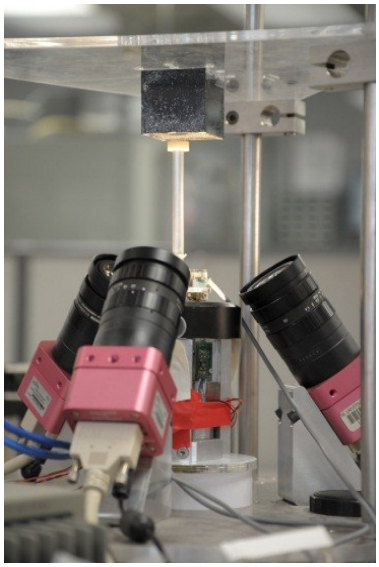

Fig. 3. Experimental setup showing micro-robot housed between stereoscope and Perspex box inverted above the robot probe.

D. Material Point Identification

A local template tracking method, based on Alvares [18] was used in this study. A speckle pattern was applied to the exposed surface of the gel phantom using an airbrush, providing a random pattern with high spatial frequency.

The material point tracking algorithm builds on work by Helm et al [19], but extends the tracking to multiple cameras, removes reference bias cameras and introduces a phase-based cross-correlation method for point identification. A region of interest (ROI) was selected by the user and triangulated from each camera. This region was defined using the corners of the acrylic box, and refined using the Harris corner finding algorithm. This ensured that pattern finding techniques were constrained to within the ROI.

The surface of the gel near the indenter was assumed to be planar when in the non-deformed state. A plane was defined by the triangulated coordinates of the corners found in the ROI. This plane was split into an even grid in 3D space. As the beginning surface was assumed to be planar, the grid points were taken as the 3D coordinates of the material points

E. Material Tracking

To measure the deformation field on the surface of the gel, material points identified in the previous section must tracked throughout the deformation.

Starting in the undeformed state, each grid point was projected onto the three cameras. A window size of 32 x 32 pixels was placed around its camera coordinates in each camera. The same windows were then placed in the images at the next displacement.

The material point was identified in the subsequent window using a novel phase-based cross correlation method. This method first uses an amplitude spectrum method in the frequency domain to identify the shift in two signals, down to half a sample space of the signals (0.5 pixels). Phase spectrum information is then used to examine the slope of a cross-correlation of the shifted signal, providing up to a twentieth of a pixel resolution [20]. This two-step method is necessary, as the spectrum wraps between $-\pi$ and π, limiting phase estimates to signal shifts less than 1 sample space. For more detail see Azhar [21].

Reconstructions of the surface geometry were compared to photos of the gel under similar loading. The deformation vectors were also compared to the original photos, and points in close proximity to the indenter tip were compared to the indenter depth.

The 3D locations of material points were plotted with respect to their initial positions, lying on the XY plane.

III. Results

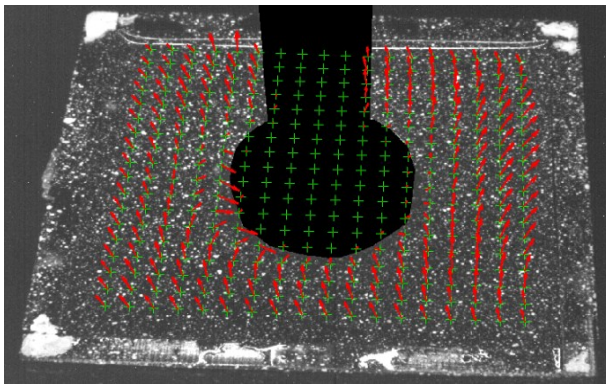

Fig. 4. Section of a 3D material point grid projected onto a camera. Green points show original position of material points, while red arrows show an exaggerated vector of material movement. Blacked out area shows the segmented out indenter tip.

A. Surface Profiling

Figure 4 shows the 3D construction of material points, forward projected onto each camera's view for the undeformed and a single deformed state. Red crosshairs show original position, while green show the deformed state. The points are overlaid onto a deformed image for comparison.

B. Tracked deformations

Figure 5 presents a side photograph of the surface profile

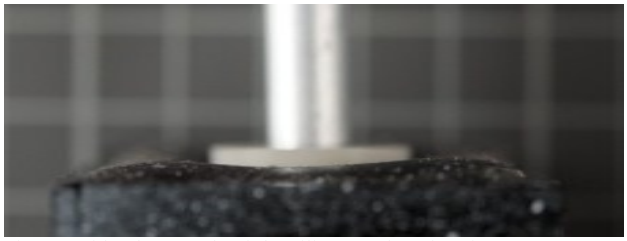

Fig. 5. Side photograph of the silicone gel surface in response to an indentation. Thick line traces the edge of the acrylic box, while the thin line traces the silicone surface that extends beyond the box.

that extends beyond the Perspex box. Bulges are clearly seen between the indenter and the corners.

Figure 6 also shows a decreasingly negative vertical displacement as material points sit at an increasing radius from the indenter, leading to bulges above the initial surface

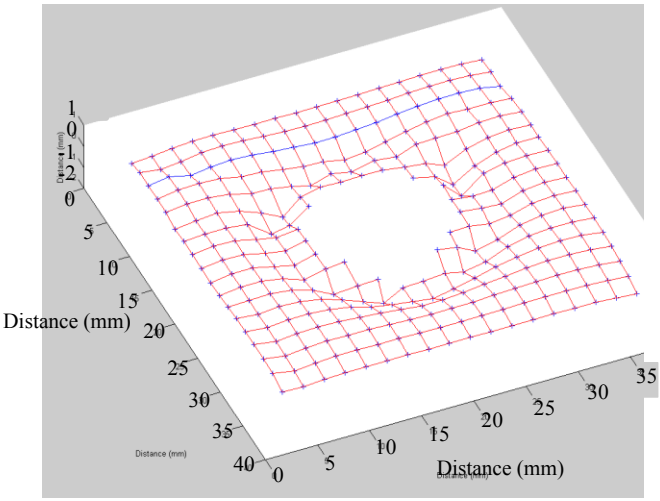

Fig. 6. Reconstruction of the silicone surface. Dots represent the tracked material points while the blue line shows a profile across the gel.

approximately half way between the indenter and corners. Points that lie directly under the indenter are removed from the results.

An initial validation of the phase tracking algorithm was performed on a separate gel sample by embedding 500 µm diameter aluminum oxide spheres onto the gel surface. The positions of the spheres were digitized both prior to and after indentation. The resulting displacements were compared to those obtained from applying the tracking algorithm to predict the deformed sphere locations using the undeformed digitized sphere locations as the tracking landmarks. Twenty spheres were tracked with a displacement error of 62 µm, 40 µm and 100 µm in the X, Y and Z directions respectively with a 1 mm indentation depth. The validation was limited by the manual digitization accuracy of the spheres which was on the order of 30 to 40 µm. Future work will look at improving the validation framework.

IV. Discussion

Initial results show promising reconstructions of a deforming soft tissue phantom. A qualitative analysis suggests that the material points identified by the surface profiling algorithm are tracked appropriately over 100um step indentations of the surface. Visibly, the blue line in figure 6 appears to reflect the real-world deformation pattern seen in figure 5.

The displacement of material points near the indenter mimic its vertical displacement, material points near the edges of the Perspex box undergo little displacement, while bulges above the surface are seen between the corners of the Perspex and indenter. This pattern can be expected, as the Perspex and indenter provide zero-displacement boundary conditions, while the open surface of the gel is the only area

in which the gel can move in response to the indenter, assuming the gel is incompressible.

Estimates of the deformation show vertical displacements >1 mm near the indenter tip when the indenter was extended 3 mm into the silicone.

As silicone phantoms have successfully been used to mimic soft tissues [15–17], we hope that there will be little difficulty applying this deformation measurement technique to human skin. However, the multiple layered nature of skin will provide different deformation patterns to that seen in an isotropic, homogeneous gel. A closer phantom may be made by layering an elastic membrane atop the silicone gel and reproducing the indentation tests.

If this approach is to be used to gain information on the anisotropy of the tissue, deformation tests other than normal indentation must be performed. Earlier work by the authors has shown successful tracking of an artificial in-plane deformation of a printed planar surface using the technique presented in this paper, while improving accuracy over non-phase-based cross-correlation methods [21]. The ability of the microrobot to perform complex deformation profiles, including in-plane deformation lends itself to multiple test scenarios of the tracking algorithm.

Deformation data obtained from these tests will be used to drive finite element models, which should allow for the identification of the mechanical properties.

Improved accuracy might result if the initial surface profile is not assumed to be planar. It is the authors' intention to utilize a surface profiling algorithm previously developed for a simpler tracking algorithm [18]. In this method the surface is assumed to be composed of as many planes or "subsets" as there are grid points. The position and orientation of each subset is identified using a non-linear optimization approach, producing a representation that is closer to the true geometry of the initial surface.

ACKNOWLEDGEMENTS

The authors would like to thank Martyn, P. Nash and Adam Reeve for their valuable contributions to this paper.

REFERENCES

[1] C. H. Daly, "Biomechanical properties of dermis.," *The Journal of investigative dermatology*, vol. 79 Suppl 1, p. 17s-20s, Jul. 1982.

[2] D. Schneider, *Viscoelasticity and tearing strength of the human skin*. Dissertation, University of California, 1982.

[3] Y. Har-Shai et al., "Mechanical Properties and Microstructure of the Superficial Musculoaponeurotic System," *Plastic and Reconstructive Surgery*, vol. 98, no. 1, 1996.

[4] F. H. Silver, J. W. Freeman, and D. DeVore, "Viscoelastic properties of human skin and processed dermis.," *Skin research and technology : official journal of International Society for Bioengineering and the Skin (ISBS) [and] International Society for Digital Imaging of Skin (ISDIS) [and] International Society for Skin Imaging (ISSI)*, vol. 7, no. 1, pp. 18-23, Feb. 2001.

[5] Y. Kvistedal and P. Nielsen, "Estimating material parameters of human skin in vivo," *Biomechanics and Modeling in Mechanobiology*, vol. 8, no. 1, pp. 1-8, Feb. 2009.

[6] D. A. Lott-Crumpler and H. R. Chaudhry, "Optimal patterns for suturing wounds of complex shapes to foster healing," *Journal of Biomechanics*, vol. 34, no. 1, pp. 51-58, Jan. 2001.

[7] M. I. Cacou C, "Effects of plane mechanical forces in wound healing in humans," *J R Coll Surg Edinb*, vol. 40, no. 1, pp. 38-41, 1995.

[8] G. L. Wilkes, I. A. Brown, and R. H. Wildnauer, "The biomechanical properties of skin.," *CRC critical reviews in bioengineering*, vol. 1, no. 4, pp. 453-495, Aug. 1973.

[9] W. A. WA., "Biaxial tension test of human skin in vivo.," *Biomed Mater Eng.*, vol. 4, no. 7, pp. 473-86, 1994.

[10] A. Delalleau, G. Josse, J.-M. Lagarde, H. Zahouani, and J.-M. Bergheau, "Characterization of the mechanical properties of skin by inverse analysis combined with the indentation test," *Journal of Biomechanics*, vol. 39, no. 9, pp. 1603-1610, 2006.

[11] C. Pailler-Mattei, S. Bec, and H. Zahouani, "In vivo measurements of the elastic mechanical properties of human skin by indentation tests," *Medical Engineering & Physics*, vol. 30, no. 5, pp. 599-606, Jun. 2008.

[12] C. Flynn, A. Taberner, and P. Nielsen, "Mechanical characterisation of in vivo human skin using a 3D force-sensitive micro-robot and finite element analysis.," *Biomechanics and modeling in mechanobiology*, vol. 10, no. 1, pp. 27-38, Feb. 2011.

[13] C. Flynn, A. Taberner, and P. Nielsen, "Measurement of the force–displacement response of in vivo human skin under a rich set of deformations," *Medical Engineering & Physics*, vol. 33, no. 5, pp. 610-619, Jun. 2011.

[14] F. Kahlesz, C. Lilge, and R. Klein, "Easy – to – Use Calibration of Multiple – Camera Setups," in *5th International Conference on Computer Vision Systems (ICVS 2007)*, 2007, no. Icvs.

[15] S. Dokos, I. J. LeGrice, B. H. Smaill, J. Kar, and A. A. Young, "A Triaxial-Measurement Shear-Test Device for Soft Biological Tissues," *Journal of Biomechanical Engineering*, vol. 122, no. 5, pp. 471-478, Oct. 2000.

[16] A. E. Kerdok, S. M. Cotin, M. P. Ottensmeyer, A. M. Galea, R. D. Howe, and S. L. Dawson, "Truth cube: Establishing physical standards for soft tissue simulation," *Medical Image Analysis*, vol. 7, no. 3, pp. 283-291, Sep. 2003.

[17] T. P. Babarenda Gamage, V. Rajagopal, M. Ehrgott, M. P. Nash, and P. M. F. Nielsen, "Identification of mechanical properties of heterogeneous soft bodies using gravity loading," *International Journal for Numerical Methods in Biomedical Engineering*, vol. 27, no. 3, pp. 391-407, 2011.

[18] D. Alvares, "A 3D Strain Measurement System for Soft Material : Application to Material Parameter Estimation," The University of Auckland, 2009.

[19] S. R. M. and M. A. S. Jeffrey D. Helm, "Improved three-dimensional image correlation for surface displacement measurement," *Opt. Eng.*, vol. 35, p. 1911, 1996.

[20] D. T. K. Malcolm, P. M. F. Nielsen, P. J. Hunter, and P. G. Charette, "Strain measurement in biaxially loaded inhomogeneous, anisotropic elastic membranes," *Biomechanics and Modeling in Mechanobiology*, vol. 1, no. 3, pp. 197-210, Dec. 2002.

[21] M. Azhar, A. Taberner, M. P. Nash, and P. M. F. Nielsen, "3D Material Point Tracking Using Phase Based Cross-Correlation Stereoscopy," in *Twenty-sixth International Conference on Image and Vision Computing New Zealand IVCNZ*, 2011.